HHS Public Access

Author manuscript

Dev Cell. Author manuscript; available in PMC 2016 April 20.

Published in final edited form as:

Dev Cell. 2015 April 20; 33(2): 176–188. doi:10.1016/j.devcel.2015.02.011.

BORC, a Multisubunit Complex that Regulates Lysosome Positioning

Jing Pu[1], **Christina Schindler**[1], **Rui Jia**[1], **Michal Jarnik**[1], **Peter Backlund**[2], and **Juan S. Bonifacino**[1,*]

[1]Cell Biology and Metabolism Program, Eunice Kennedy Shriver National Institute of Child Health and Human Development, National Institutes of Health, Bethesda, MD 20892, USA

[2]Biomedical Mass Spectrometry Facility, Eunice Kennedy Shriver National Institute of Child Health and Human Development, National Institutes of Health, Bethesda, MD 20892, USA

SUMMARY

The positioning of lysosomes within the cytoplasm is emerging as a critical determinant of many lysosomal functions. Here we report the identification of a multi-subunit complex named BORC that regulates lysosome positioning. BORC comprises eight subunits, some of which are shared with the BLOC-1 complex involved in the biogenesis of lysosome-related organelles, and the others of which are products of previously uncharacterized open reading frames. BORC associates peripherally with the lysosomal membrane, where it functions to recruit the small GTPase Arl8. This initiates a chain of interactions that promotes the Kinesin-1-dependent movement of lysosomes toward the plus ends of microtubules in the peripheral cytoplasm. Interference with BORC or other components of this pathway results in collapse of the lysosomal population into the pericentriolar region. In turn, this causes reduced cell spreading and migration, highlighting the importance of BORC-dependent centrifugal transport for non-degradative functions of lysosomes.

INTRODUCTION

Lysosomes are membrane-enclosed organelles whose main function is the degradation of biomacromolecules delivered by way of endocytosis, phagocytosis, autophagy, or biosynthetic transport (Saftig and Klumperman, 2009). In addition, lysosomes participate in various other cellular processes, including microbial killing, antigen presentation, detoxification, cholesterol homeostasis, apoptosis, metabolic signaling, exosome release, plasma membrane repair, cell migration, and cancer invasion and metastasis (Saftig and Klumperman, 2009). Recent evidence indicates that at least some of these processes are

*Correspondence: bonifacinoj@helix.nih.gov.

SUPPLEMENTAL INFORMATION

Supplemental Information includes Supplemental Experimental Procedures, four figures, two tables, and one movie and can be found with this article online at http://dx.doi.org/10.1016/j.devcel.2015.02.011.

AUTHOR CONTRIBUTIONS

J.P., C.S., and J.S.B. conceived the project. J.P. performed most of the experiments. C.S. performed the initial affinity purifications, R.J. performed cell spreading and migration assays, M.J. performed electron microscopy, and P.B. performed MS of recombinant BORC. All authors analyzed the data. J.P. and J.S.B. wrote the manuscript, and the other authors edited it.

influenced by the positioning of lysosomes within the cytoplasm (Steffan et al., 2010; Korolchuk et al., 2011; Garg et al., 2011). Two spatially distinct populations of lysosomes have been observed: a juxta-nuclear cluster centered on the microtubule-organizing center (MTOC) and peripheral vesicles scattered throughout the cytoplasm. This distribution is highly dynamic because lysosomes move bidirectionally between both populations along microtubule tracks (Matteoni and Kreis, 1987). Centripetal (inward) movement is regulated by the small GTPase Rab7 and its effector RILP, which recruit the minus end-directed microtubule motor Dynein-Dynactin to lysosomes (Cantalupo et al., 2001; Jordens et al., 2001). The opposite process, centrifugal (outward) movement, is mediated by another small GTPase, Arl8, and its effector SKIP, which link lysosomes to the plus end-directed microtubule motor Kinesin-1 (also known as conventional kinesin, a KLC_2-$KIF5_2$ heterotetramer) (Hofmann and Munro, 2006; Bagshaw et al., 2006; Dumont et al., 2010; Rosa-Ferreira and Munro, 2011).

Arl8 is a member of the Arf family of small GTPases, which are characterized by having an N-terminal amphipathic α helix (Gillingham and Munro, 2007). A distinctive feature of Arl8 is that this helix is N-terminally acetylated, in contrast to most other Arf family members, in which the helix is N-terminally myristoylated (Hofmann and Munro, 2006). Importantly, of the ~30 members of the Arf family in humans (Gillingham and Munro, 2007), two paralogs of Arl8 (Arl8a and Arl8b) are the only ones known to associate specifically with lysosomes (Hofmann and Munro, 2006; Bagshaw et al., 2006; Rosa-Ferreira and Munro, 2011; Garg et al., 2011). The N-terminal helix of Arl8 is required for recruitment to membranes, although not specifically to lysosomes (Hofmann and Munro, 2006). Therefore, other interactions must specify lysosomal targeting of Arl8.

We obtained unexpected insights into the mechanism of Arl8 recruitment to lysosomes in the course of our studies on Hermansky-Pudlak syndrome (HPS). HPS is an autosomal recessive disordercharacterized by defects in the biogenesis of various lysosome-related organelles (LROs), including melanosomes and platelet dense bodies (Dell'Angelica, 2004). To date, this disorder has been shown to result from mutations in at least nine different genes in humans and 15 genes in mice. Most of the proteins encoded by these genes are components of four multisubunit complexes named adaptor protein 3 (AP-3) and biogenesis of lysosome-related organelles complex 1, 2, and 3 (BLOC-1, 2, and 3) (Dell'Angelica, 2004). AP-3 functions as an adaptor protein to sort transmembrane cargos to LROs, as is best demonstrated for the sorting of tyrosinase to melanosomes (Theos et al., 2005). The molecular functions of the BLOCs are less well understood. BLOC-1 is the most complex of all, comprising eight subunits named BLOS1, BLOS2, BLOS3, pallidin, Snapin, muted, cappuccino, and dysbindin (Falcón-Pérez et al., 2002; Moriyama and Bonifacino, 2002; Starcevic and Dell'Angelica, 2004; Lee et al., 2012). Another protein named KXD1 has been shown recently to interact with BLOC-1 subunits, although at present it is unclear whether this protein is a core component of the complex (Yang et al., 2012).

In an effort to identify proteins that interact with BLOC-1, we discovered a related multisubunit complex named BORC (BLOC-one-related complex). BORC comprises three subunits common to BLOC-1 (BLOS1, BLOS2, and Snapin) plus KXD1 and four previously uncharacterized proteins (LOH12CR1/myrlysin, C17orf59/lyspersin, C10orf32/

diaskedin, and MEF2BNB). Remarkably, clustered regularly interspaced short palindromic repeats (CRISPR) knockout (KO) or siRNA knockdown (KD) of BORC subunits in HeLa cells caused dissociation of Arl8b from lysosomes and collapse of the peripheral lysosome population into the pericentriolar region. This redistribution of lysosomes was due to inhibition of their centrifugal movement along microtubules. In contrast, depletion of the BLOC-1-specific subunits had no effect on Arl8b localization or lysosome positioning/motility. We conclude that BORC functions to recruit Arl8 to lysosomes, thereby initiating a chain of interactions that promotes microtubule-guided transport of lysosomes toward the cell periphery.

RESULTS

Identification of Proteins that Co-purify with BLOS2

To identify proteins that interact with the BLOC-1 complex, we performed tandem affinity purification (TAP) followed by mass spectrometry (MS) using detergent extracts from human HeLa cells stably expressing the BLOS2 subunit of BLOC-1 appended with an N-terminal One-STrEP/FLAG (OSF) tag. Only proteins that were isolated from two independent BLOS2-expressing clones and not from untransfected cells (Table S1) were considered for further analysis. Among the specifically isolated proteins were the eight subunits of BLOC-1 (BLOS1, BLOS2, BLOS3, pallidin, Snapin, muted, cappuccino, and dysbindin) (Falcón-Pérez et al., 2002; Moriyama and Bonifacino, 2002; Starcevic and Dell'Angelica, 2004; Lee et al., 2012; Figure 1A; Table S1). Other specific interactors identified in this analysis were several proteins reported previously to bind to BLOC-1, including KXD1 (Yang et al., 2012) and subunits of the AP-3 complex (AP3D1, AP3B2, and AP3M1) (Di Pietro et al., 2006; Gokhale et al., 2012; Figure 1A; Table S1). We also found previously unreported interactors, including the five subunits of Ragulator (LAMTOR1–5; Table S1), a multimeric complex that regulates activation of the target of rapamycin complex 1 (mTORC1) kinase at the lysosomal membrane (Bar-Peled et al., 2012). Another set of interactors comprised four uncharacterized proteins denoted LOH12CR1, C17orf59, C10orf32, and MEF2BNB that, overall, were as abundant as the BLOC-1 subunits in the BLOS2 isolates (Figure 1A; Table S1). These proteins caught our attention because they had a small size (~12–37 kDa) (Figure 1B) and predicted coiled-coil regions (Figure S1A) similar to the BLOC-1 subunits (Dell'Angelica, 2004). Furthermore, mRNA expression data in the GeneCards database (http://www.genecards.org) indicated that LOH12CR1, C17orf59, C10orf32, and MEF2BNB were ubiquitously expressed in human tissues, as is also the case for BLOC-1 subunits (Falcón-Pérez et al., 2002; Moriyama and Bonifacino, 2002; Starcevic and Dell'Angelica, 2004). Immunoblot analysis using an antibody to the predicted LOH12CR1 protein confirmed that this protein was expressed in multiple mammalian tissues and cell lines (Figure S1B). These similarities prompted us to examine in more detail the relationship of these uncharacterized proteins to BLOC-1.

Phylogenetic analyses using the position-specific iterated BLAST (PSI-BLAST) algorithm (http://blast.ncbi.nlm.nih.gov/Blast.cgi) identified orthologs of BLOC-1 subunits (particularly BLOS1, BLOS2, and Snapin) among members of most eukaryotic supergroups (Figure S1C; Cheli and Dell'Angelica, 2010; Hayes et al., 2011). Orthologs of LOH12CR1,

C17orf59, C10orf32, MEF2BNB, and KXD1 had a more limited distribution to metazoans and a few eukaryotic supergroups (Figure S1C). PSI-BLAST analyses did not reveal a homology of these four proteins to any other known protein, but the more sensitive HHpred tool (toolkit.tuebingen.mpg.de/hhpred) detected a weak homology of LOH12CR1 to *S. cerevisiae* Snn1p (a Snapin homolog) and C17orf59 to *S. cerevisiae* Cnl1p (a cappuccino homolog), both components of a yeast BLOC-1-like complex (Hayes et al., 2011). This finding reinforced the notion that these proteins could be subunits of BLOC-1 or of a related complex.

To further explore the connection of these proteins to BLOC-1, we performed a TAP-MS analysis using several clones of human H4 cells expressing LOH12CR1 or C17orf59 tagged with One-STrEP/FLAG at either the N terminus (OSF) or C terminus (FLAG-One-STrEP) (Figure 1A). In all cases, we found that both proteins co-purified with each other, as well as with C10orf32, MEF2BNB and KXD1 (Figure 1A). They also co-purified with BLOS1, BLOS2, and Snapin but not (or to a much lesser extent) with BLOS3, muted, dysbindin, cappuccino, and pallidin (Figure 1A). These observations led us to hypothesize that LOH12CR1, C17orf59, C10orf32, MEF2BNB, KXD1, BLOS1, BLOS2, and Snapin were subunits of a distinct multimeric complex that we named “BLOC-one-related complex” (BORC) (Figure 1C). For reasons that will become apparent in the following sections, we renamed LOH12CR1 “myrlysin” (myristoylated lysosomal protein), C17orf59 “lyspersin” (for lysosome-dispersing protein), and C10orf32 “diaskedin” (from the Ancient Greek “diaskedazo,” meaning “to disperse”) (Figure 1C).

Biochemical Characterization of BORC

To test for the existence of distinct BLOC-1 and BORC complexes in HeLa cells, we performed immunoprecipitation of cell extracts with antibodies to endogenous myrlysin (unique to BORC), pallidin (unique to BLOC-1), and Snapin (common to both complexes), followed by immunoblotting with antibodies to the same proteins. Indeed, we observed that the antibody to myrlysin co-precipitated Snapin but not pallidin, whereas the antibody to pallidin co-precipitated Snapin but not myrlysin (Figure 2A). In line with these findings, the antibody to Snapin co-precipitated both myrlysin and pallidin (Figure 2A). Because we did not have a suitable set of antibodies to other BLOC-1 and BORC subunits, we used a similar protocol with HeLa cells stably expressing Myc-, OSF-, or FOS-tagged subunits. After isolation of the tagged subunits with anti-Myc or StrepTactin beads, blots were probed with antibodies to myrlysin or Snapin (Figure 2B). These experiments showed that endogenous myrlysin co-isolated with tagged lyspersin, diaskedin, MEF2BNB, KXD1, Snapin, BLOS1, and BLOS2 but not with tagged BLOS3, dysbindin, muted, cappuccino, and pallidin. Endogenous Snapin co-isolated with all of the tagged subunits (Figure 2B).

Confirmation of the composition of BORC was obtained by co-expression of its eight putative subunits from a single polycistronic expression plasmid in *E. coli*, as done previously for BLOC-1 (Lee et al., 2012; Figure 2C). The purified proteins were analyzed by gel filtration, followed by SDS-PAGE, Coomassie blue staining, and MS of the individual bands (Figure 2C). All eight proteins were readily identified in the gels (Table S2), with lyspersin migrating as a triplet (likely because of partial proteolysis) and diaskedin

and MEF2BNB migrating at the same position (Figure 2C). Importantly, all proteins exhibited the same elution profile, peaking at a position corresponding to a Stokes radius (Rh) of ~78 Å (Figure 2C). The elution behavior of the recombinant complex was similar to that of the endogenous complex in H4 cell extracts detected by immunoblotting for myrlysin (Figure 2D), indicating that all BORC subunits were likely accounted for in our biochemical analyses. Both recombinant and endogenous BORC eluted slightly later (peaking in fraction 30) than endogenous BLOC-1 identified by immunoblotting for pallidin (fractions 28–29) (Figures 2C and 2D). BORC therefore appeared smaller or less asymmetric than BLOC-1. Endogenous Snapin showed a broader maximum that spanned the BLOC-1 and BORC peaks (Figure 2D), consistent with it being a subunit of both complexes.

Finally, we examined the biogenetic interdependence of the BORC and BLOC-1 subunits by performing small interfering RNA (siRNA)-mediated KD of the different subunits and immunoblotting for myrlysin and pallidin (Figure 2E). Overall, we observed that KD of BORC-specific subunits reduced the levels of myrlysin but not pallidin (Figure 2D). In contrast, KD of BLOC-1-specific subunits reduced the levels of pallidin but not myrlysin (Figure 2D). KD of the shared subunits reduced both myrlysin and pallidin (Figure 2D). Taken together, these experiments demonstrated the existence of a distinct BORC complex comprising three subunits shared with BLOC-1 plus KXD1 and four unique subunits (Figure 1C).

BORC Regulates Lysosome Positioning

We next investigated the intracellular localization and function of BORC. Because the antibody to myrlysin did not detect the endogenous protein by immunofluorescence microscopy, we expressed myrlysin-FOS or myrlysin-GFP by transfection in HeLa cells. These constructs exhibited either a diffuse cytoplasmic distribution or, at higher expression levels, an association with vacuoles that co-stained for co-expressed Snapin-HA and the late endosomal/lysosomal markers LysoTracker and Lamp-1 (Figures S2A and S2B) but not the early/recycling endosomal transferrin receptor (TfR) (data not shown). Because late endosomes and lysosomes share many properties, for simplicity we will henceforth refer to them indistinctly as “lysosomes.” The association of myrlysin and Snapin with lysosomes was supported by a recent proteomic analysis of rat lysosomes that detected myrlysin, lyspersin, diaskedin, KXD1, Snapin, BLOS1, and BLOS2 among 734 proteins identified in the analysis (Chapel et al., 2013). Notably, pallidin, cappuccino, muted, dysbindin, and BLOS3 were absent from the lysosomal fraction (Chapel et al., 2013). Therefore, BORC, but not BLOC-1 (Di Pietro et al., 2006), localizes to lysosomes.

The Myristoylator program (web.expasy.org/myristoylator) predicted that the myrlysin N-terminal sequence MGSEQSSEA is myristoylated at the glycine residue. Indeed, metabolic labeling showed incorporation of [^{3}H]-myristic acid into myrlysin-FOS but not a myrlysin-G2A-FOS construct having a substitution of the N-terminal glycine by alanine (Figure S2C). Importantly, although myrlysin-FOS localized to lysosomes (Figures S2A and S2B), myrlysin-G2A-FOS exhibited a diffuse cytosolic distribution (Figure S2D), indicating that myristoylation is required for the association of myrlysin with lysosomes.

To investigate a possible role of BORC in connection to lysosomes, we used the CRISPR/Cas9 system to ablate all copies of the myrlysin gene in HeLa cells (Figure 3A). Immunoblot analysis using two antibodies to the endogenous protein confirmed that the KO cells expressed no myrlysin (Figure 3B). Immunostaining for lysosomal proteins such as Lamp-1, CD63, and LAMTOR4 revealed a striking phenotypic difference. Although lysosomes were mostly scattered throughout the cytoplasm in wild-type (WT) cells, they were tightly clustered in the juxtanuclear region in myrlysin-KO cells (Figures 3C and 3D). Electron microscopy (EM) analysis showed that lysosomes remained as individual vesicles and had an apparently normal size and morphology in myrlysin-KO cells (Figures S2E–S2G). In contrast, immunostaining with antibodies to the TfR and labeling with MitoTracker (mitochondria) and ER-Tracker (ER) showed no difference in the distribution of other cytoplasmic organelles in myrlysin-KO cells relative to WT cells (Figure 3C). Transient (Figure 3E) or stable (Figure S3A) transfection of the mutant cells with a plasmid encoding myrlysin-GFP restored the normal distribution of lysosomes and revealed co-localization of myrlysin-GFP with Lamp-1 on cytoplasmic foci as well as structures found near the plasma membrane, particularly at cell protrusions. From these results we concluded that myrlysin associates with lysosomes and promotes their dispersal to the cell periphery.

BORC Recruits Arl8b to Lysosomes

The lysosome-positioning defect of the myrlysin-KO cells was reminiscent of that resulting from interference with the Arl8b-SKIP-Kinesin-1 pathway (Bagshaw et al., 2006; Hofmann and Munro, 2006; Rosa-Ferreira and Munro, 2011; Figure 4A). Biochemical analyses indeed showed co-isolation of Arl8b-GFP, Myc-SKIP, kinesin light chain (KLC)-GFP, and KIF5-GFP on StrepTactin pull-downs from myrlysin-FOS-expressing but not control cells, consistent with a direct or indirect interaction of BORC with all of these proteins (Figure 4B).

The findings above prompted us to examine the distribution of Arl8b-GFP expressed in WT and myrlysin-KO HeLa cells. Interestingly, we found that although Arl8b-GFP localized to Lamp-1-positive structures in WT cells, it exhibited a mostly diffuse distribution in myrlysin-KO cells (Figure 4C). Another small GTPase, Rab7-GFP, remained associated with late endosomes/lysosomes in myrlysin-KO cells despite the clustering of these organelles in the juxtanuclear region (Figure 4D). Treatment of HeLa cells with siRNAs to myrlysin, lyspersin, Snapin, KXD1, BLOS1, or BLOS2 also caused juxtanuclear clustering of lysosomes and complete or partial dissociation of Arl8b-GFP into the cytosol (Figure 5). KD of diaskedin and MEF2BNB had no visible effect on either property (Figure 5), possibly because they are not essential for the function of the complex or because the extent of KD was insufficient. In contrast to the results for most BORC subunits, KD of the BLOC-1-specific pallidin, cappuccino, muted, BLOS3, and dysbindin did not affect lysosome and Arl8b-GFP distribution (Figure 5). The differential effects of knocking down BORC-specific and BLOC-1-specific subunits were also observed in the H4 cell line (Figure S3B). Together, these experiments indicate that BORC, but not BLOC-1, promotes lysosome dispersal through recruitment of Arl8b to the lysosomal membrane.

BORC Enables Kinesin-1-Dependent Movement of Lysosomes toward the Cell Periphery

To further test the involvement of BORC in the Arl8b-SKIP-Kinesin-1 pathway (Figure 4A), we examined the effect of overexpressing Myc-SKIP on the distribution of lysosomes in WT and myrlysin-KO HeLa cells. We observed that, in WT cells, SKIP overexpression shifted lysosomes to the cell periphery, particularly to cell protrusions or vertices (Figure 6A), as described previously (Dumont et al., 2010; Rosa-Ferreira and Munro, 2011). In myrlysin-KO cells, however, SKIP overexpression had little or no effect on lysosome distribution (Figure 6A). This finding is consistent with the requirement of BORC and Arl8b recruitment for SKIP function. We also examined the effect of expressing a Lamp-1-GFP construct containing three copies of the KLC-binding sequence (KBS) TNLEWDDSAI from SKIP (Pernigo et al., 2013). This construct, which bypasses BORC, Arl8b, and SKIP in linking lysosomes to Kinesin-1, caused peripheral accumulation of lysosomes in both WT and myrlysin-KO cells (Figure 6B). These findings support the notion that BORC acts upstream of Arl8b in a pathway for lysosome dispersal.

To ascertain that the role of BORC on lysosome positioning-involved regulation of organelle motility, we performed live-cell imaging of Lamp-1-GFP in WT and myrlysin-KO HeLa cells (Movie S1; Figure 6C). We observed that, in WT cells, lysosomes exhibited long-range movement in both anterograde and retrograde directions (Figure 6C). Movement was most frequent along tracks running from the juxtanuclear region to cell vertices known to contain the plus ends of microtubules. Lysosomes occasionally became tubular as they were pulled toward the cell periphery (Movie S1). In contrast, in myrlysin-KO cells, there was virtually no long-range transport of lysosomes, and their movements were limited to jiggling motions within the juxtanuclear cluster (Movie S1; Figure 6C). Moreover, no tubular lysosomes were observed in the myrlysin-KO cells (Movie S1). Therefore, BORC engages the Arl8b-SKIP-Kinesin-1 pathway to regulate centrifugal movement and tubulation of lysosomes.

BORC-Dependent Lysosome Movement Regulates Cell Spreading and Migration

What are the physiological consequences of defective lysosome dispersal in BORC-deficient cells? Despite their juxtanuclear clustering in myrlysin-KO HeLa cells, lysosomes contained the acid hydrolase cathepsin D (Figures S3C and S3D) and were able to degrade internalized DQ-BSA (a fluid-phase lysosomal proteolysis sensor) (Figure S3E). The regulation of mTORC1 by starvation and refeeding also appeared normal in myrlysin-KO cells (Figure S4A). However, myrlysin-KO cells had elevated levels of lipidated LC3 (Figures S4B and S4C), suggesting a defect in autophagy downstream from mTORC1. In addition, myrlysin-KO cells seemed smaller than WT cells, as was best appreciated upon highlighting of the cell borders with phalloidin-Alexa 488 (Figure 7A). Quantification by image analysis showed a significant reduction (~30%) of the footprint area of myrlysin-KO cells relative to WT cells (Figure 7B). Stable expression of myrlysin-GFP in myrlysin-KO cells restored the footprint area to that of the WT cells (Figures 7A and 7B). In contrast, forward-scatter analysis by flow cytometry of cells in suspension (a measure of cell diameter) showed no difference in size among WT, myrlysin-KO, and myrlysin-GFP-rescued cells (Figure 7C). Therefore, myrlysin-KO appears to cause a defect in cell spreading.

Transport of late endosomes or lysosomes to the cell periphery is required for delivery of cell adhesion regulators during cell migration (Dozynkiewicz et al., 2012; Schiefermeier et al., 2014). Indeed, two-dimensional cell migration analysis using a circular gap closure assay (Figure 7D) showed that the migration velocity of myrlysin-KO cells was reduced ~50% relative to WT and myrlysin-GFP-rescued cells (Figures 7D and 7E). Similar reductions in cell spreading and migration were observed upon KD of Arl8b in HeLa cells, a manipulation that also caused clustering of lysosomes in the juxtanuclear region (Figures S4D–S4I). None of these changes were due to differences in cell proliferation; all of these cell lines exhibited similar doubling times of ~22 hr (Figures S4J and S4K). These experiments therefore revealed an important physiological requirement of BORC-dependent lysosome dispersal for the regulation of cell spreading and motility.

DISCUSSION

Our studies have identified a multisubunit complex named BORC as a key component of the molecular machinery that regulates lysosome positioning. BORC acts at an early stage, recruiting Arl8b to the lysosomal membrane and therefore enabling coupling to the SKIP-Kinesin-1 complex that drives microtubule-guided movement of lysosomes toward the cell periphery (Hofmann and Munro, 2006; Bagshaw et al., 2006; Dumont et al., 2010; Rosa-Ferreira and Munro, 2011). BORC is also required for the formation of tubular lysosomes, which, likewise, depends on Arl8b and SKIP (Mrakovic et al., 2012). We considered the possibility that BORC functions as a guanine nucleotide exchange factor (GEF) for Arl8b. However, we were unable to detect GEF activity of recombinant BORC on Arl8b using well established in vitro assays (data not shown). This negative result could be due to the lack of an additional component or post-translational modification of BORC. Alternatively, BORC might not be an Arl8 GEF but, rather, an adaptor for an Arl8 GEF or a receptor that specifies recruitment of Arl8 to lysosomes.

The function of BORC in promoting Arl8-SKIP-Kinesin-1-dependent centrifugal transport of lysosomes counters the role of the Rab7-RILP-Dynein-Dynactin complex in mediating lysosome transport in the opposite direction (Cantalupo et al., 2001, Jordens et al., 2001). Interestingly, Rab7 can also promote centrifugal transport of autophagosomes, and probably late endosomes and lysosomes, through recruitment of another effector, FYCO1 (Pankiv et al., 2010). The specific kinesin involved in this transport, however, has not been identified. In addition to Kinesin-1, other candidates are Kinesin-2 (KIF3A; Brown et al., 2005), Kinesin-3 (KIF1Bβ3; Matsushita et al., 2004), and Kinesin-13 (KIF2β; Santama et al., 1998), which also promote centrifugal transport of lysosomes in some settings. The mechanisms that control the positioning of lysosomes and related organelles are therefore complex and, likely, subject to coordinate regulation in response to different physiological stimuli.

Although BORC and BLOC-1 share the BLOS1, BLOS2, and Snapin subunits (and perhaps KXD1 as well; Yang et al., 2012), the cellular processes in which these complexes participate appear to be different. Unlike BORC, BLOC-1 is not associated with lysosomes (Chapel et al., 2013; Di Pietro et al., 2006), and its KD does not cause changes in Arl8b recruitment and lysosome positioning. BLOC-1 is instead known to participate in the

biogenesis of LROs such as melanosomes and platelet dense bodies (Dell'Angelica, 2004), although the molecular mechanisms involved remain unclear. We speculate that, by analogy to BORC, BLOC-1 might function to couple another organelle to a microtubule motor in the process of LRO biogenesis. In this regard, immunoelectron microscopy studies have revealed the presence of BLOC-1 on endosome-derived tubules in the proximity of melanosomes (Di Pietro et al., 2006). These tubules have also been shown to contain the adaptor protein complex AP-1 and another kinesin, KIF13A, both of which are required for peripheral positioning of recycling endosomal domains involved in melanosome biogenesis (Delevoye et al., 2009). It remains to be determined, however, whether all of these proteins work together in a molecular mechanism analogous to that of BORC and its downstream effectors.

Humans and mice with inactivating mutations of BLOC-1-specific subunits (BLOS3, pallidin, muted, cappuccino, or dysbindin) are viable despite severe defects in various LROs (Dell'Angelica, 2004). In contrast, a Snapin-KO mouse is perinatally inviable (Tian et al., 2005), in part because of defective brain development (Zhou et al., 2011). Furthermore, KO of the BLOS1 gene in mice causes embryonic lethality at stage embryonic day (E) 12.5 (Zhang et al., 2014). The lethal phenotypes of the Snapin and BLOS1 KO mice can now be explained by the fact that these proteins are subunits of both BLOC-1 and BORC. Perhaps BORC is more important than BLOC-1 or both complexes have partly overlapping functions in supporting viability. *C. elegans* Snapin mutants are viable but exhibit defects in the biogenesis of gut granules (a type of LRO) (Hermann et al., 2012) and the synaptic vesicle cycle (Yu et al., 2013).

Snapin was originally identified as a protein that interacts with the target-soluble N-ethylmaleimide attachment protein receptor (t-SNARE) SNAP-25 and modulates neurotransmitter release. Since then, Snapin has been ascribed many other functions, including the regulation of endolysosomal trafficking and autophagy in neurons (Cai et al., 2010). Although these studies have focused on Snapin independent of its role in any multisubunit complex, it is likely that the reported functions are attributable to BORC, BLOC-1, or both. An apparent difference between previous studies and our study is that Snapin has been proposed to mediate Dynein-driven retrograde transport of late endosomes in neurons (Cai et al., 2010), whereas we found that BORC promotes Kinesin-1-driven anterograde transport in non-neuronal cells. Further studies will be needed to determine whether Snapin has functions independent of BORC or whether BORC mediates microtubule-guided transport in both directions depending on the cell type or other conditions.

BORC might participate in other processes shown previously to involve Arl8 and/or SKIP. For example, in *C. elegans* coelomocytes, Arl8 is required for fusion of late endosomes and phagosomes with lysosomes (Nakae et al., 2010; Sasaki et al., 2013). In mammalian cells, Arl8b was also implicated in phagosome-lysosome fusion, microbial killing, and antigen processing and presentation (Garg et al., 2011). These functions may depend on the ability of Arl8b to deploy lysosomes to the peripheral cytoplasm so that they meet incoming endocytic or phagocytic organelles. Both Arl8b and SKIP also regulate the polarization and cytotoxic function of lytic granules (a type of LRO) in natural killer cells (Tuli et al., 2013).

Finally, Arl8 regulates the transport of synaptic vesicle precursors down the axon in *C. elegans* neurons (Wu et al., 2013). In light of our findings, it would be of interest to determine whether BORC functions upstream of Arl8 in all of these processes.

The ability to move lysosomes to the cell periphery is likely important for an even broader range of cellular functions. For example, we have shown that myrlysin-KO cells exhibit reduced spreading and motility. This phenotype may arise from the involvement of late endosomes and lysosomes in the delivery of adhesion molecules (e.g., integrins; Dozynkiewicz et al., 2012), signaling scaffolds (e.g., Ragulator; Schiefermeier et al., 2014), and acid hydrolases (e.g., Cathepsin B; Steffan et al., 2010) to the plasma membrane or the extracellular space. We have indeed observed clustering of lysosomes at cell protrusions or vertices that may correspond to focal adhesion or cell motility structures. This peripheral clustering of lysosomes is dependent on BORC (this study) and is also subject to control by Arl8b and SKIP (Rosa-Ferreira and Munro, 2011). Because of the critical importance of cell adhesion and motility in tumor growth, invasion, and metastasis, the BORC-Arl8b-SKIP-Kinesin-1 pathway of lysosome dispersal could be an attractive target for pharmacologic inhibition in cancer therapeutics.

EXPERIMENTAL PROCEDURES

Cell Culture, Transfection, and RNAi

HeLa and H4 cells were cultured in DMEM supplemented with 10% fetal bovine serum (FBS) at 37°C and 5% CO_2. Plasmid transfection was performed using Lipofectamine 2000 (Life Technologies). The plasmids used in this study are listed in the Supplemental Information. For transient expression, cells were analyzed 48–72 hr after transfection. For RNAi experiments, cells were transfected twice with a 48-hr interval with siRNA pools or non-targeting control siRNA (GE Healthcare) using Oligofectamine (Life Technologies) and analyzed 6 days after seeding.

Tandem Affinity Purification and Mass Spectrometry

HeLa and H4 cells stably expressing proteins tagged with N-terminal OSF or C-terminal FOS were lysed in 50 mM Tris-HCl (pH 7.4), 300 mM NaCl, 5 mM EDTA, and 1% Triton X-100 supplemented with proteinase inhibitor cocktail (Roche). Cell lysates were cleared by centrifugation at 17,000 × *g* for 15 min and incubated with StrepTactin resin (IBA) for 1 hr at 4°C. Bound proteins were eluted with 2.5 mM desthiobiotin after washing with 50 mM Tris-HCl (pH 7.4), 300 mM NaCl, 5 mM EDTA, and 0.2% Triton X-100. Proteins were further purified using FLAG antibody-coated beads (Sigma) eluted with 150 ng/ml 3× FLAG peptide (Sigma). Proteins were precipitated with 10% trichloroacetic acid (TCA), washed with acetone, air-dried, and analyzed by liquid chromatography (LC)/MS at the Taplin MS facility (Harvard Medical School).

Preparation of Recombinant BORC and Size-Exclusion Chromatography

Codon-optimized BORC subunit cDNAs were cloned into a modified polycistronic expression plasmid, pST39 (Lee et al., 2012; Figure 2C). A hexahistidine (His_6) tag was inserted at the N terminus of Snapin and a GST tag at the C terminus of myrlysin, both

separated from the corresponding protein by a tobacco etch virus (TEV) protease cleavage site. Recombinant BORC was produced in *E. coli* and sequentially purified on nickel-nitrilotriacetic acid (Ni-NTA) resin and glutathione resin (GE Healthcare).

Recombinant BORC was analyzed by size-exclusion chromatography on Superose 6 (GE Healthcare), and fractions were subjected to SDS-PAGE and Coomassie blue staining. Individual bands were identified by MS. The Stokes radius of recombinant BORC was determined by comparison with standard proteins run on the same column (Sigma). To analyze the gel filtration behavior of endogenous BORC and BLOC-1, H4 cell extracts were similarly analyzed on Superose 6. Fractions were collected and precipitated with 10% TCA. Precipitated proteins were analyzed by SDS-PAGE and immunoblotting. Additional details on recombinant BORC production and characterization are described in the Supplemental Experimental Procedures.

CRISPR/Cas9 Knockout

We inactivated the myrlysin gene using the CRISPR/Cas9 system (Cong et al., 2013). Briefly, two 20-base pair (bp) targeting sequences (GCTCAACAG CATGCTGCCCG and AGCAGATCCAGAAAGTGAAC) were synthesized (Eurofins) and introduced separately into the px330 plasmid (Addgene). HeLa cells were co-transfected with both plasmids and re-seeded after 72 hr to allow single colony formation. After 12 days, genomic DNA was extracted from individual colonies, and cleavage of the target sequence was tested by PCR using a pair of primers (ATCTGCGGGACTGTGTCCCT and CAGATTTTCAT GCCAGCCGG), which produced a 99-bp smaller band in KO cells relative to WT cells. The KO was confirmed by Sanger sequencing and immunoblotting.

To generate myrlysin-GFP-rescued cells and proper control cells, retrovirus particles were prepared by transfecting HEK293T cells with the pQCXIP-myrlysin-GFP or pQCXIP-GFP plasmid and retrovirus packaging plasmids (Clontech Laboratories). Stably transduced cells were selected with 2 μg/ml puromycin.

Immunofluorescence Microscopy and Live-Cell Imaging

Cells were cultured on fibronectin-coated coverslips, fixed with 4% paraformaldehyde, and permeabilized with 0.2% Triton X-100. Primary antibodies and Alexa-conjugated secondary antibodies diluted in 0.2% BSA-containing PBS were used to probe specific proteins. A list of antibodies used and their sources is shown in the Supplemental Information. Alexa-conjugated Phalloidin (Life Technologies) was used to stain for F-actin. Coverslips were mounted on glass slides with Fluoromount-G (EMS) and examined on a Zeiss LSM710 confocal microscope).

For live-cell imaging, cells were seeded on fibronectin-coated Lab-Tek chambers (Thermo Scientific) and transfected with the indicated plasmids. MitoTracker or ER-Tracker (Life Technologies) were used according to the manufacturer's instructions. Live-cell imaging was performed using a Zeiss LSM710 confocal microscope equipped with Definite Focus and an environmental chamber set at 37°C and 5% CO_2.

Cell Migration

Cells were seeded on Radius cell migration plates (Cell Biolabs) and allowed to form monolayers for 20 hr. Circular gaps were generated by removing the gels. Cells were kept in an incubator at 37°C, and phase-contrast images were captured at different times (from 0–30 h). The gap area was analyzed using ImageJ. Cell migration velocity was calculated and statistically analyzed from three to five independent experiments.

Statistical Methods

All pooled data are presented as the mean ± SD from at least three independent experiments. Two-tailed Student's t test for unpaired data was used to evaluate single comparisons between different experimental groups using Microsoft Excel. Differences were considered statistically significant at a value of $p < 0.05$.

Other Methods

Additional methods are described in the Supplemental Experimental Procedures.

Supplementary Material

Refer to Web version on PubMed Central for supplementary material.

Acknowledgments

We thank X. Zhu and N. Tsai for expert technical assistance; E. Dell'Angelica, J. Brumell, and S. Méresse for the kind gifts of reagents; X. Ren, S.Y. Park, and M. Machner for help with some experimental procedures; and D. Gershlick and R. Mattera for critical comments on the manuscript. This work was funded by the Intramural Program of NICHD, NIH (ZIA HD001607).

References

Bagshaw RD, Callahan JW, Mahuran DJ. The Arf-family protein, Arl8b, is involved in the spatial distribution of lysosomes. Biochem Biophys Res Commun. 2006; 344:1186–1191. [PubMed: 16650381]

Bar-Peled L, Schweitzer LD, Zoncu R, Sabatini DM. Ragulator is a GEF for the rag GTPases that signal amino acid levels to mTORC1. Cell. 2012; 150:1196–1208. [PubMed: 22980980]

Brown CL, Maier KC, Stauber T, Ginkel LM, Wordeman L, Vernos I, Schroer TA. Kinesin-2 is a motor for late endosomes and lysosomes. Traffic. 2005; 6:1114–1124. [PubMed: 16262723]

Cai Q, Lu L, Tian JH, Zhu YB, Qiao H, Sheng ZH. Snapin-regulated late endosomal transport is critical for efficient autophagy-lysosomal function in neurons. Neuron. 2010; 68:73–86. [PubMed: 20920792]

Cantalupo G, Alifano P, Roberti V, Bruni CB, Bucci C. Rab-interacting lysosomal protein (RILP): the Rab7 effector required for transport to lysosomes. EMBO J. 2001; 20:683–693. [PubMed: 11179213]

Chapel A, Kieffer-Jaquinod S, Sagné C, Verdon Q, Ivaldi C, Mellal M, Thirion J, Jadot M, Bruley C, Garin J, et al. An extended proteome map of the lysosomal membrane reveals novel potential transporters. Mol Cell Proteomics. 2013; 12:1572–1588. [PubMed: 23436907]

Cheli VT, Dell'Angelica EC. Early origin of genes encoding subunits of biogenesis of lysosome-related organelles complex-1, -2 and -3. Traffic. 2010; 11:579–586. [PubMed: 20102546]

Cong L, Ran FA, Cox D, Lin S, Barretto R, Habib N, Hsu PD, Wu X, Jiang W, Marraffini LA, Zhang F. Multiplex genome engineering using CRISPR/Cas systems. Science. 2013; 339:819–823. [PubMed: 23287718]

Delevoye C, Hurbain I, Tenza D, Sibarita JB, Uzan-Gafsou S, Ohno H, Geerts WJ, Verkleij AJ, Salamero J, Marks MS, Raposo G. AP-1 and KIF13A coordinate endosomal sorting and positioning during melanosome biogenesis. J Cell Biol. 2009; 187:247–264. [PubMed: 19841138]

Dell'Angelica EC. The building BLOC(k)s of lysosomes and related organelles. Curr Opin Cell Biol. 2004; 16:458–464. [PubMed: 15261680]

Di Pietro SM, Falcón-Pérez JM, Tenza D, Setty SR, Marks MS, Raposo G, Dell'Angelica EC. BLOC-1 interacts with BLOC-2 and the AP-3 complex to facilitate protein trafficking on endosomes. Mol Biol Cell. 2006; 17:4027–4038. [PubMed: 16837549]

Dozynkiewicz MA, Jamieson NB, Macpherson I, Grindlay J, van den Berghe PV, von Thun A, Morton JP, Gourley C, Timpson P, Nixon C, et al. Rab25 and CLIC3 collaborate to promote integrin recycling from late endosomes/lysosomes and drive cancer progression. Dev Cell. 2012; 22:131–145. [PubMed: 22197222]

Dumont A, Boucrot E, Drevensek S, Daire V, Gorvel JP, Poüs C, Holden DW, Méresse S. SKIP, the host target of the Salmonella virulence factor SifA, promotes kinesin-1-dependent vacuolar membrane exchanges. Traffic. 2010; 11:899–911. [PubMed: 20406420]

Falcón-Pérez JM, Starcevic M, Gautam R, Dell'Angelica EC. BLOC-1, a novel complex containing the pallidin and muted proteins involved in the biogenesis of melanosomes and platelet-dense granules. J Biol Chem. 2002; 277:28191–28199. [PubMed: 12019270]

Garg S, Sharma M, Ung C, Tuli A, Barral DC, Hava DL, Veerapen N, Besra GS, Hacohen N, Brenner MB. Lysosomal trafficking, antigen presentation, and microbial killing are controlled by the Arf-like GTPase Arl8b. Immunity. 2011; 35:182–193. [PubMed: 21802320]

Gillingham AK, Munro S. The small G proteins of the Arf family and their regulators. Annu Rev Cell Dev Biol. 2007; 23:579–611. [PubMed: 17506703]

Gokhale A, Larimore J, Werner E, So L, Moreno-De-Luca A, Lese-Martin C, Lupashin VV, Smith Y, Faundez V. Quantitative proteomic and genetic analyses of the schizophrenia susceptibility factor dys-bindin identify novel roles of the biogenesis of lysosome-related organelles complex 1. J Neurosci. 2012; 32:3697–3711. [PubMed: 22423091]

Hayes MJ, Bryon K, Satkurunathan J, Levine TP. Yeast homologues of three BLOC-1 subunits highlight KxDL proteins as conserved interactors of BLOC-1. Traffic. 2011; 12:260–268. [PubMed: 21159114]

Hermann GJ, Scavarda E, Weis AM, Saxton DS, Thomas LL, Salesky R, Somhegyi H, Curtin TP, Barrett A, Foster OK, et al. C. elegans BLOC-1 functions in trafficking to lysosome-related gut granules. PLoS ONE. 2012; 7:e43043. [PubMed: 22916203]

Hofmann I, Munro S. An N-terminally acetylated Arf-like GTPase is localised to lysosomes and affects their motility. J Cell Sci. 2006; 119:1494–1503. [PubMed: 16537643]

Jordens I, Fernandez-Borja M, Marsman M, Dusseljee S, Janssen L, Calafat J, Janssen H, Wubbolts R, Neefjes J. The Rab7 effector protein RILP controls lysosomal transport by inducing the recruitment of dynein-dynactin motors. Curr Biol. 2001; 11:1680–1685. [PubMed: 11696325]

Korolchuk VI, Saiki S, Lichtenberg M, Siddiqi FH, Roberts EA, Imarisio S, Jahreiss L, Sarkar S, Futter M, Menzies FM, et al. Lysosomal positioning coordinates cellular nutrient responses. Nat Cell Biol. 2011; 13:453–460. [PubMed: 21394080]

Lee HH, Nemecek D, Schindler C, Smith WJ, Ghirlando R, Steven AC, Bonifacino JS, Hurley JH. Assembly and architecture of biogenesis of lysosome-related organelles complex-1 (BLOC-1). J Biol Chem. 2012; 287:5882–5890. [PubMed: 22203680]

Matsushita M, Tanaka S, Nakamura N, Inoue H, Kanazawa H. A novel kinesin-like protein, KIF1Bbeta3 is involved in the movement of lysosomes to the cell periphery in non-neuronal cells. Traffic. 2004; 5:140–151. [PubMed: 15086790]

Matteoni R, Kreis TE. Translocation and clustering of endosomes and lysosomes depends on microtubules. J Cell Biol. 1987; 105:1253–1265. [PubMed: 3308906]

Moriyama K, Bonifacino JS. Pallidin is a component of a multi-protein complex involved in the biogenesis of lysosome-related organelles. Traffic. 2002; 3:666–677. [PubMed: 12191018]

Mrakovic A, Kay JG, Furuya W, Brumell JH, Botelho RJ. Rab7 and Arl8 GTPases are necessary for lysosome tubulation in macrophages. Traffic. 2012; 13:1667–1679. [PubMed: 22909026]

Nakae I, Fujino T, Kobayashi T, Sasaki A, Kikko Y, Fukuyama M, Gengyo-Ando K, Mitani S, Kontani K, Katada T. The arf-like GTPase Arl8 mediates delivery of endocytosed macromolecules to lysosomes in Caenorhabditis elegans. Mol Biol Cell. 2010; 21:2434–2442. [PubMed: 20484575]

Pankiv S, Alemu EA, Brech A, Bruun JA, Lamark T, Overvatn A, Bjørkøy G, Johansen T. FYCO1 is a Rab7 effector that binds to LC3 and PI3P to mediate microtubule plus end-directed vesicle transport. J Cell Biol. 2010; 188:253–269. [PubMed: 20100911]

Pernigo S, Lamprecht A, Steiner RA, Dodding MP. Structural basis for kinesin-1:cargo recognition. Science. 2013; 340:356–359. [PubMed: 23519214]

Rosa-Ferreira C, Munro S. Arl8 and SKIP act together to link lysosomes to kinesin-1. Dev Cell. 2011; 21:1171–1178. [PubMed: 22172677]

Saftig P, Klumperman J. Lysosome biogenesis and lysosomal membrane proteins: trafficking meets function. Nat Rev Mol Cell Biol. 2009; 10:623–635. [PubMed: 19672277]

Santama N, Krijnse-Locker J, Griffiths G, Noda Y, Hirokawa N, Dotti CG. KIF2beta, a new kinesin superfamily protein in non-neuronal cells, is associated with lysosomes and may be implicated in their centrifugal translocation. EMBO J. 1998; 17:5855–5867. [PubMed: 9774330]

Sasaki A, Nakae I, Nagasawa M, Hashimoto K, Abe F, Saito K, Fukuyama M, Gengyo-Ando K, Mitani S, Katada T, Kontani K. Arl8/ARL-8 functions in apoptotic cell removal by mediating phagolysosome formation in Caenorhabditis elegans. Mol Biol Cell. 2013; 24:1584–1592. [PubMed: 23485564]

Schiefermeier N, Scheffler JM, de Araujo ME, Stasyk T, Yordanov T, Ebner HL, Offterdinger M, Munck S, Hess MW, Wickström SA, et al. The late endosomal p14-MP1 (LAMTOR2/3) complex regulates focal adhesion dynamics during cell migration. J Cell Biol. 2014; 205:525–540. [PubMed: 24841562]

Starcevic M, Dell'Angelica EC. Identification of snapin and three novel proteins (BLOS1, BLOS2, and BLOS3/reduced pigmentation) as subunits of biogenesis of lysosome-related organelles complex-1 (BLOC-1). J Biol Chem. 2004; 279:28393–28401. [PubMed: 15102850]

Steffan JJ, Williams BC, Welbourne T, Cardelli JA. HGF-induced invasion by prostate tumor cells requires anterograde lysosome trafficking and activity of Na+-H+ exchangers. J Cell Sci. 2010; 123:1151–1159. [PubMed: 20215403]

Theos AC, Tenza D, Martina JA, Hurbain I, Peden AA, Sviderskaya EV, Stewart A, Robinson MS, Bennett DC, Cutler DF, et al. Functions of adaptor protein (AP)-3 and AP-1 in tyrosinase sorting from endosomes to melanosomes. Mol Biol Cell. 2005; 16:5356–5372. [PubMed: 16162817]

Tian JH, Wu ZX, Unzicker M, Lu L, Cai Q, Li C, Schirra C, Matti U, Stevens D, Deng C, et al. The role of Snapin in neurosecretion: snapin knock-out mice exhibit impaired calcium-dependent exocytosis of large dense-core vesicles in chromaffin cells. J Neurosci. 2005; 25:10546–10555. [PubMed: 16280592]

Tuli A, Thiery J, James AM, Michelet X, Sharma M, Garg S, Sanborn KB, Orange JS, Lieberman J, Brenner MB. Arf-like GTPase Arl8b regulates lytic granule polarization and natural killer cell-mediated cytotoxicity. Mol Biol Cell. 2013; 24:3721–3735. [PubMed: 24088571]

Wu YE, Huo L, Maeder CI, Feng W, Shen K. The balance between capture and dissociation of presynaptic proteins controls the spatial distribution of synapses. Neuron. 2013; 78:994–1011. [PubMed: 23727120]

Yang Q, He X, Yang L, Zhou Z, Cullinane AR, Wei A, Zhang Z, Hao Z, Zhang A, He M, et al. The BLOS1-interacting protein KXD1 is involved in the biogenesis of lysosome-related organelles. Traffic. 2012; 13:1160–1169. [PubMed: 22554196]

Yu SC, Klosterman SM, Martin AA, Gracheva EO, Richmond JE. Differential roles for snapin and synaptotagmin in the synaptic vesicle cycle. PLoS ONE. 2013; 8:e57842. [PubMed: 23469084]

Zhang A, He X, Zhang L, Yang L, Woodman P, Li W. Biogenesis of lysosome-related organelles complex-1 subunit 1 (BLOS1) interacts with sorting nexin 2 and the endosomal sorting complex required for transport-I (ESCRT-I) component TSG101 to mediate the sorting of epidermal growth factor receptor into endosomal compartments. J Biol Chem. 2014; 289:29180–29194. [PubMed: 25183008]

Zhou B, Zhu YB, Lin L, Cai Q, Sheng ZH. Snapin deficiency is associated with developmental defects of the central nervous system. Biosci Rep. 2011; 31:151–158. [PubMed: 20946101]

Highlights

- BORC is a multisubunit complex associated with the cytosolic face of lysosomes
- BORC recruits Arl8, coupling lysosomes to the plus-end microtubule motor Kinesin-1
- BORC therefore promotes the movement of lysosomes toward the peripheral cytoplasm
- BORC-dependent lysosome dispersal contributes to cell spreading and motility

A

Bait

Prey: Protein	OSF-BLOS2	OSF-BLOS2	OSF-LOH12CR1	LOH12CR1 - FOS	OSF-C17orf59	OSF-C17orf59	C17orf59 -FOS	
Muted	19	15						BLOC-1
Dysbindin	18	15				2	1	BLOC-1
Cappuccino	11	10	1					BLOC-1
Pallidin	5	3						BLOC-1
BLOS3	7	7						BLOC-1
BLOS2	14	9	5	3	6	6	3	BLOC-1 + BORC
BLOS1	11	8	3	1	7	6	7	BLOC-1 + BORC
Snapin	7	8	4	3	5	6	6	BLOC-1 + BORC
KXD1	5	7	3	2	8	8	8	BLOC-1
LOH12CR1	22	18	25	16	14	11	10	BORC
C17orf59	22	20	11	7	18	20	21	BORC
C10orf32	10	8	4	2	6	7	4	BORC
MEF2BNB	7	5			4	6	6	BORC

Number of peptides.

B

Human Protein	AA No.	Mass (kD)	Zebrafish ortholog	Drosophila ortholog	*C. Elegans* ortholog
BLOS1	153	17.1	NP_001037815	CG30077	T20G5.10
BLOS2	142	15.8	NP_001231685	CG14145	Y73B6BL.30
Snapin	136	14.9	NP_001038613	CG9958	C02B10.2
KXD1	176	19.7	AAI50447	CG10681	C13F10.2
LOH12CR1	196	22.2	XP_005163065	CG11802	F59E12.11
C17orf59	357	37.1	NP_001038453	CG17180	Y37E11B.3
C10orf32	106	11.7	NP_001035077	CG18065	R03A10.1
MEF2BNB	109	12.5	XP_005170514	CG32590	K11B4.2

C

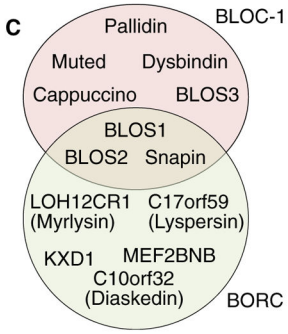

Figure 1. Proteomic Identification of BORC

(A) Proteins that interact with BLOS2, LOH12CR1, or C17orf59 appended with OSF or FOS tags were identified by TAP-MS from HeLa (BLOS2) or H4 cells (LOH12CR1 and C17orf59). Selected prey proteins and their numbers of peptides detected in the MS are shown. The results suggest the existence of two complexes, BLOC-1 and BORC, that share BLOS1, BLOS2, and Snapin. KXD1 could also be a component of BLOC-1. The possibility that there could be variants of these complexes having different subunit combinations cannot be ruled out.

(B) Properties and orthologs of BORC subunits. AA, amino acid.

(C) Schematic of the overlapping subunit composition of BLOC-1 and BORC. New names for the previously uncharacterized subunits are shown in parenthesis. See also Figure S1 and Table S1.

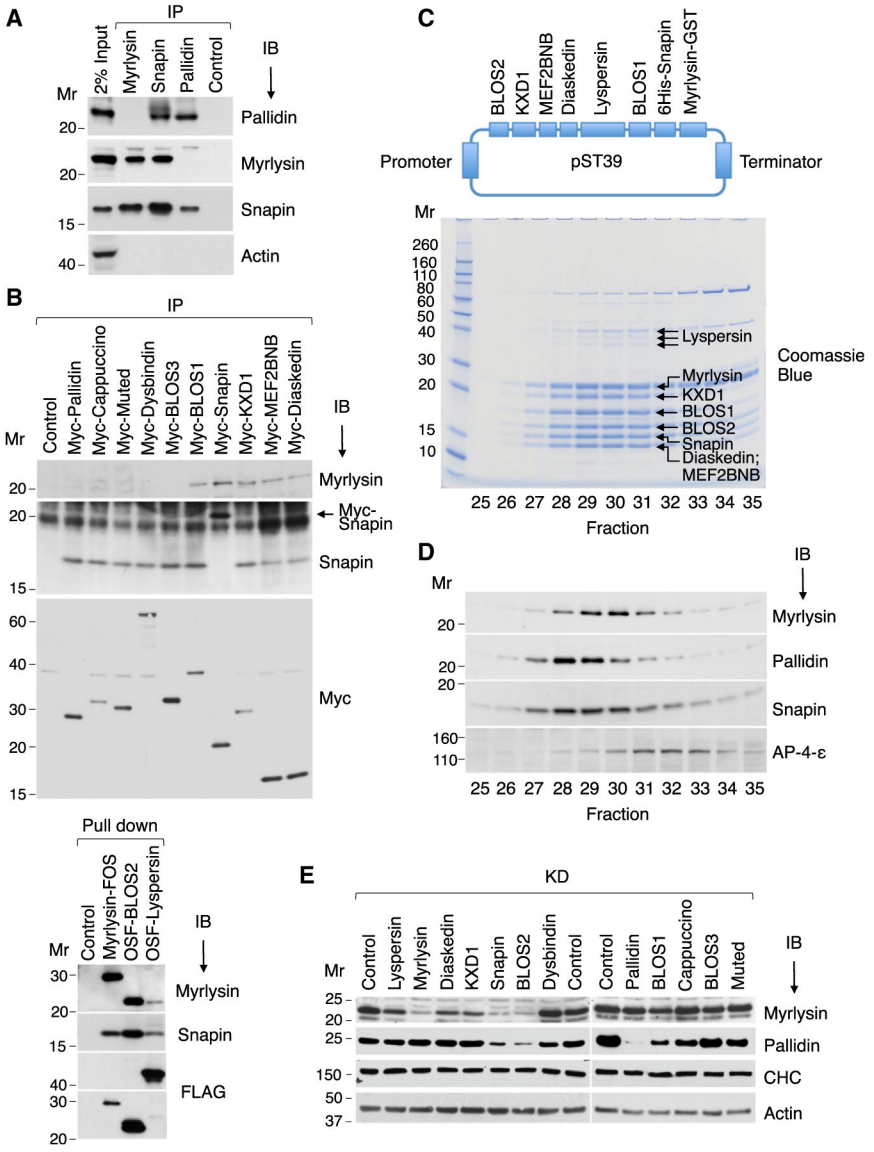

Figure 2. Biochemical Characterization of BORC

(A) HeLa cell extracts were subjected to immuno-precipitation (IP) followed by immunoblotting (IB) with the indicated antibodies.

(B) HeLa cells stably expressing Myc-, FOS-, or OSF-tagged subunits of BORC and BLOC-1 were extracted with lysis buffer and subjected to immunoprecipitation with antibody to the Myc epitope or pull-down with Strep-Tactin beads. Endogenous myrlysin and Snapin were then detected by immunoblotting. The ~20-kDa band in the Snapin IB of the Myc-Snapin IP lane (arrow) corresponds to Myc-Snapin.

(C) cDNAs encoding BORC subunits, including His_6-Snapin and myrlysin-GST, were cloned into the *E. coli* expression plasmid pST39 (top). Purified BORC was cleaved with TEV protease to remove the tags and analyzed by gel filtration on Superose 6. Fractions 25–35 were resolved by SDS-PAGE, and proteins were visualized by Coomassie blue staining (bottom) and their identity confirmed by MS (Table S2).

(D) H4 cell extracts were analyzed by gel filtration under the same conditions as in (B). Endogenous myrlysin, pallidin, Snapin, and the adaptor protein 4 (AP-4) ε subunit (control) were detected by immunoblotting.

(E) siRNA-KD of BORC and BLOC-1 subunits was performed in HeLa cells, and myrlysin, pallidin, clathrin heavy chain (CHC), and actin (the latter two as controls) were detected by immunoblotting. The positions of molecular mass (Mr) markers (in kilodaltons) are indicated.

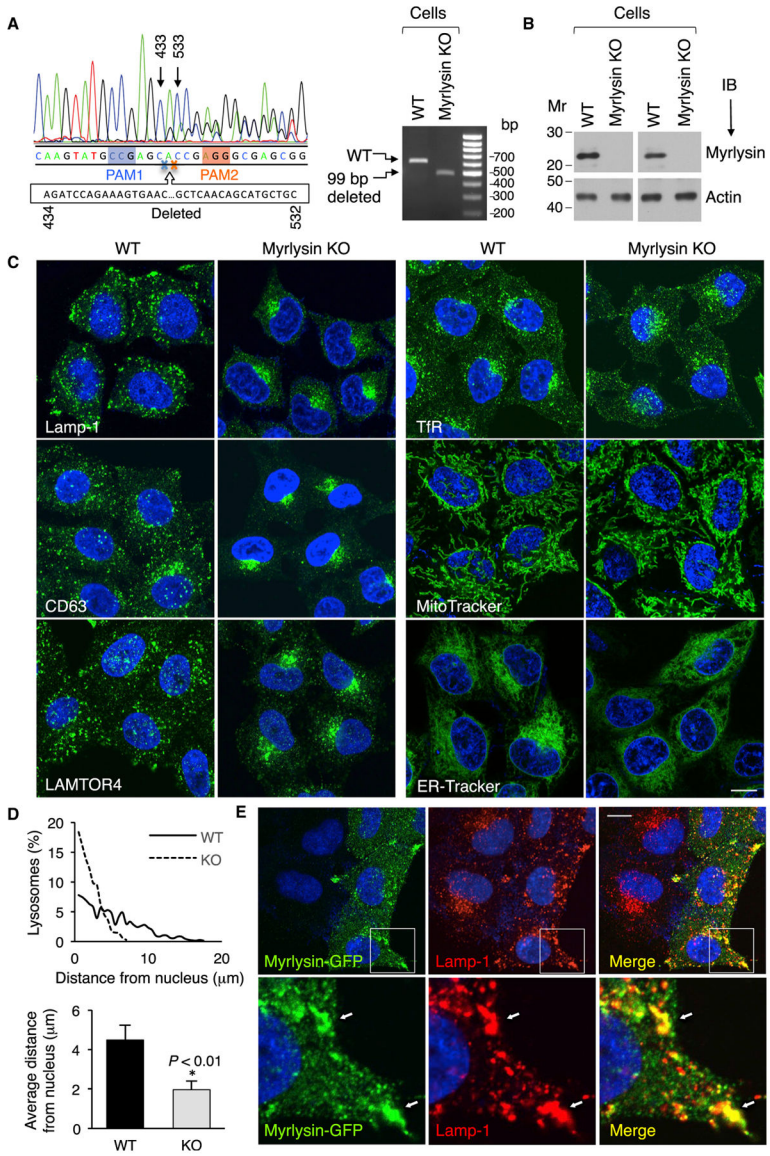

Figure 3. Myrlysin Regulates Lysosome Positioning

(A) Sanger sequencing of the genomic PCR product from a CRISPR/Cas9 myrlysin-KO HeLa cell clone shows a 99-bp deletion (residues 434–532 of cDNA) between two protospacer-adjacent motifs (PAM) (left). The agarose gel shows the PCR products from WT and myrlysin-KO cells (right).

(B) No myrlysin was detected in the KO cells by immunoblotting using antibodies to a synthetic peptide (residues 167–196) (left two lanes) or to a GST fusion protein (right two lanes).

(C) Confocal microscopy of WT and myrlysin-KO cells immunostained for Lamp-1, CD63, LAMTOR4, or TfR or stained with MitoTracker or ER-Tracker. Scale bar, 10 μm.

(D) The distance of lysosomes from the nucleus boundary in WT (solid line and black bar) and myrlysin-KO cells (dashed line and gray bar) was measured using ImageJ. Twenty-five

cells in each group were analyzed. Bar graphs represent the mean ± SD. The p value was calculated using Student's t test.

(E) myrlysin-GFP was transiently expressed in myrlysin-KO cells, and lysosomes were visualized by immunostaining with antibody to Lamp-1. Scale Bar, 10 μm. Notice the rescue of the lysosome-positioning phenotype in the myrlysin-GFP transfected but not in the untransfected cells. The bottom row shows 3.9-fold-magnified views of the insets. Arrows indicate co-localization. See also Figure S2.

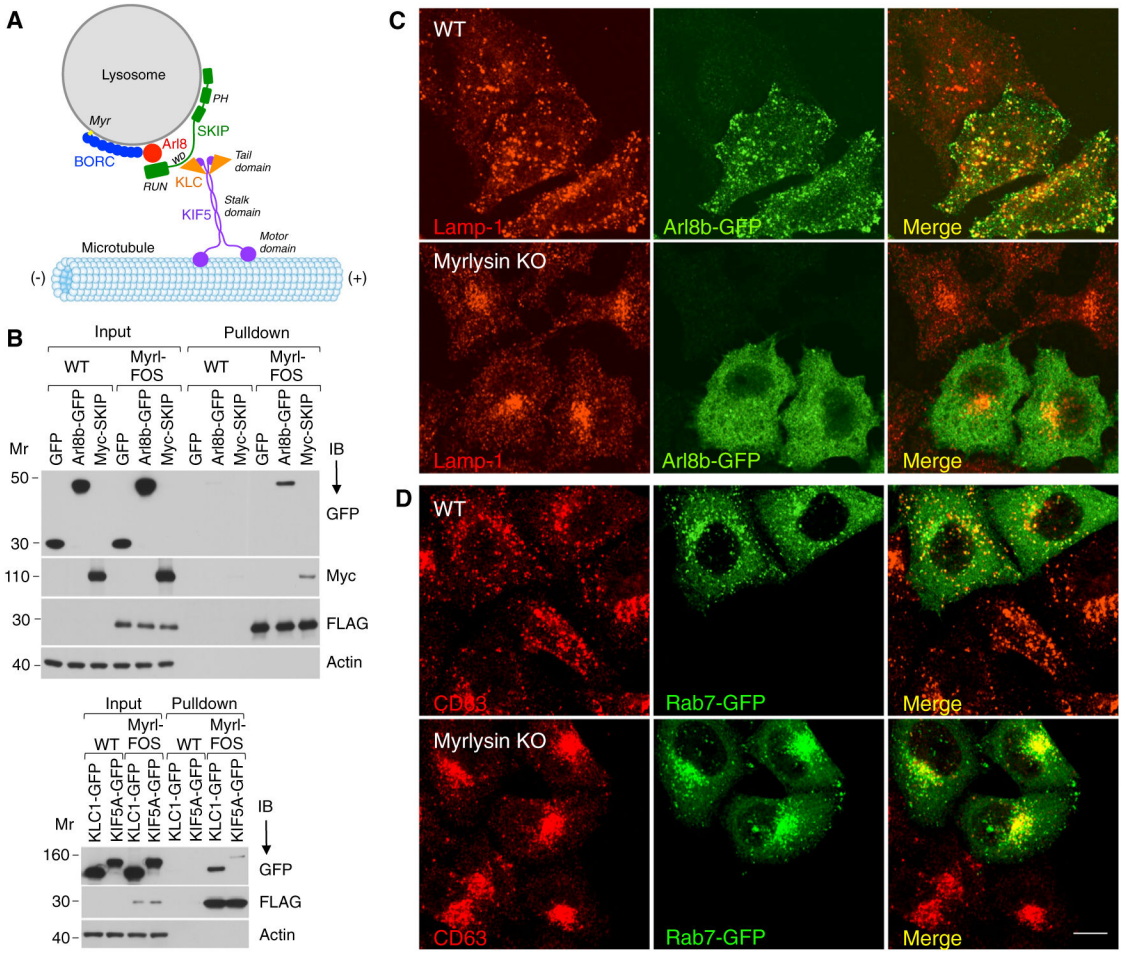

Figure 4. BORC Recruits Arl8b to Lysosomes

(A) Schematic representing the involvement of BORC in the Arl8b-SKIP-Kinesin-1 pathway of lysosome movement toward the plus end of microtubules. PH, pleckstrin homology; RUN, RPIP8, UNC-14, and NESCA.

(B) WT and myrlysin-FOS-expressing H4 cells were transiently transfected with plasmids encoding Arl8b-GFP, Myc-SKIP, KLC1-GFP, KIF5A-GFP, or GFP (control). After 72 hr, cells were treated with dithio-bis-succinimidyl propionate, extracted, and subjected to pull-down with StrepTactin beads. Eluted proteins were analyzed by immunoblotting with the indicated antibodies. myrlysin. The positions of molecular mass markers (in kilodaltons) are indicated. Myrl, myrlysin.

(C and D) Confocal microscopy of WT and myrlysin-KO HeLa cells transiently transfected with plasmids encoding Arl8b-GFP (C) or Rab7-GFP (D) and immunostained for GFP and Lamp-1 or CD63. Scale bar, 10 μm.

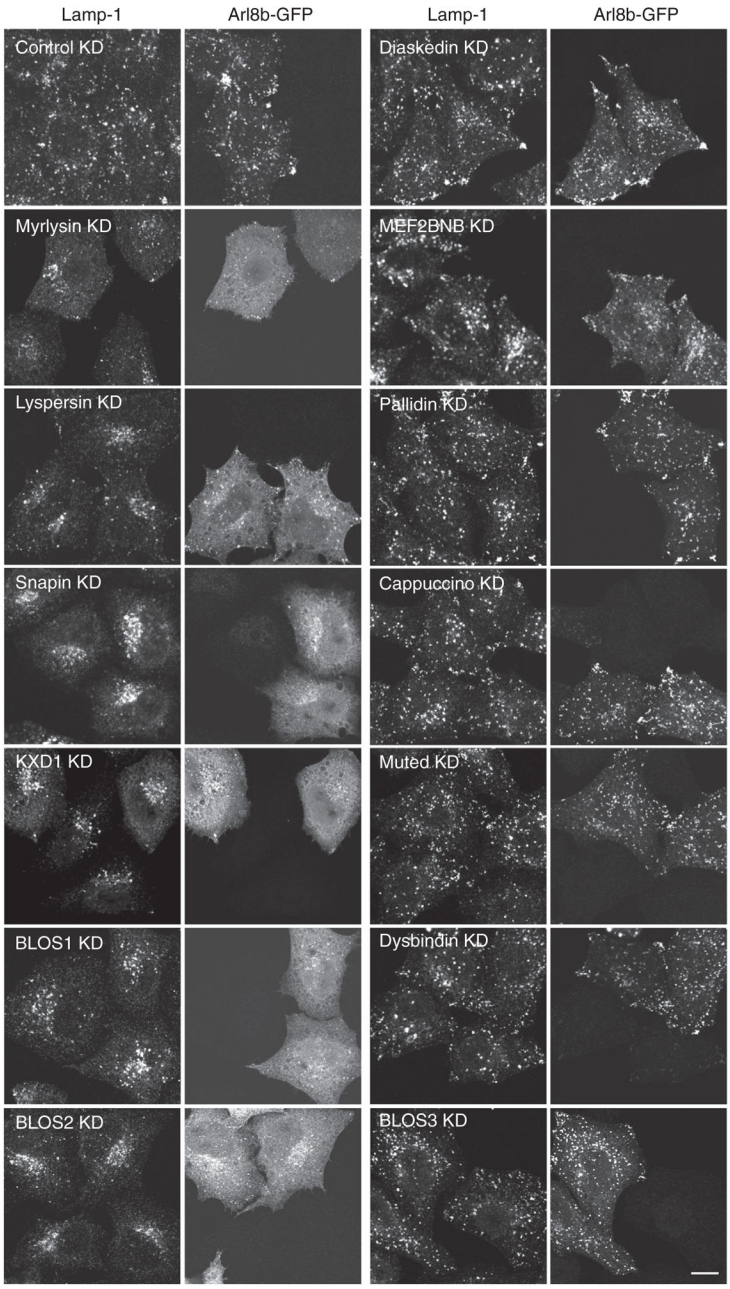

Figure 5. Requirement of BORC, but Not BLOC-1, for Lysosome Dispersal and Arl8b Recruitment

siRNA-mediated KD of BORC and BLOC-1 subunits was performed in HeLa cells. Non-targeting siRNA was used as a control. Arl8b-GFP was expressed by transfection 48 hr after KD. Fixed permeabilized cells were stained with antibodies to GFP and Lamp-1 and examined by confocal microscopy. KD of myrlysin, lyspersin, Snapin, KXD1, BLOS1, and BLOS2 resulted in juxtanuclear clustering of lysosomes and dissociation of Arl8b in 65%–90% of the cells. The extent of Arl8b dissociation in these KD cells was 84%–97% as quantified by image analysis. Scale bar, 10 μm. See also Figure S3.

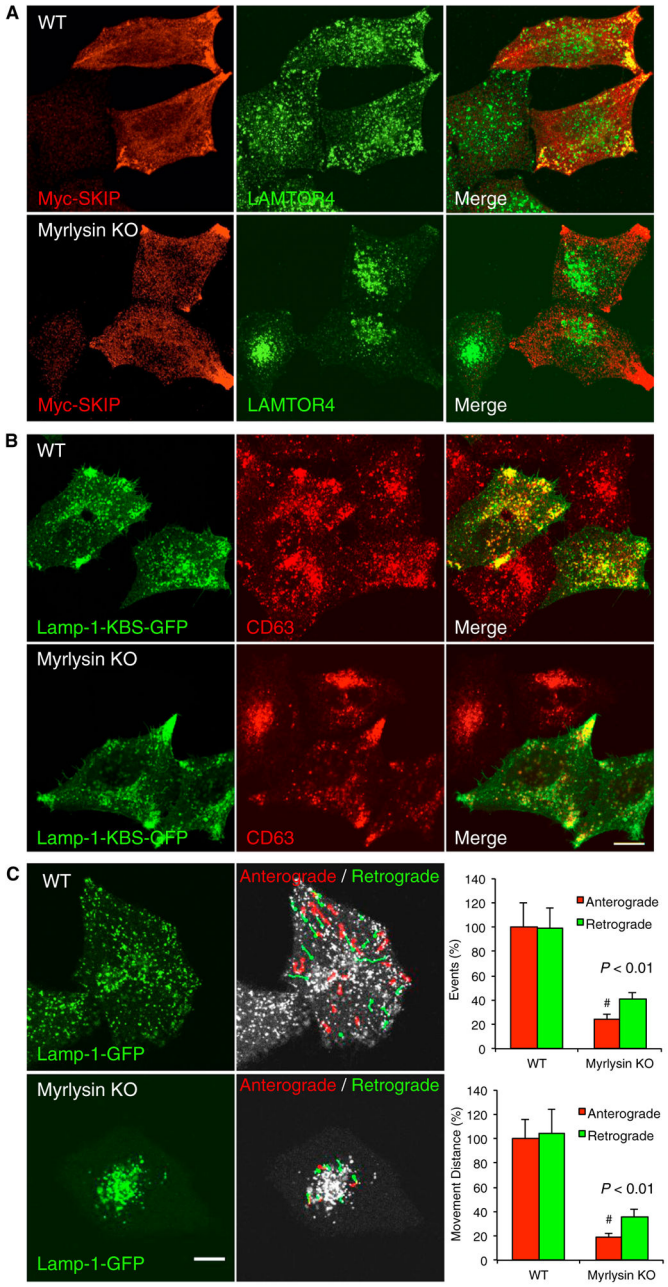

Figure 6. BORC Enables Kinesin-1-Dependent Motility of Lysosomes

(A and B) WT and myrlysin-KO HeLa cells were transiently transfected with plasmids encoding Myc-SKIP (A) or Lamp-1-KBS-GFP (B) and fixed 48 hr thereafter (KBS, KLC-binding sequence). Cells were immunostained for Myc, GFP, LAMTOR4, and/or CD63 and examined by confocal microscopy. Scale bar, 10 μm.

(C) WT and myrlysin-KO cells were transiently transfected with a plasmid encoding Lamp-1-GFP and imaged live 48 hr later. The images show the first frames from Movie S1 (left). Anterograde (red) and retrograde (green) movements were tracked using ImageJ over a 19-s period. The number and distance of lysosome movements were quantified from the

movies for five cells in each group. Values are mean ± SD. The p values were calculated using Student's t test (right). Scale bar, 5 μm.

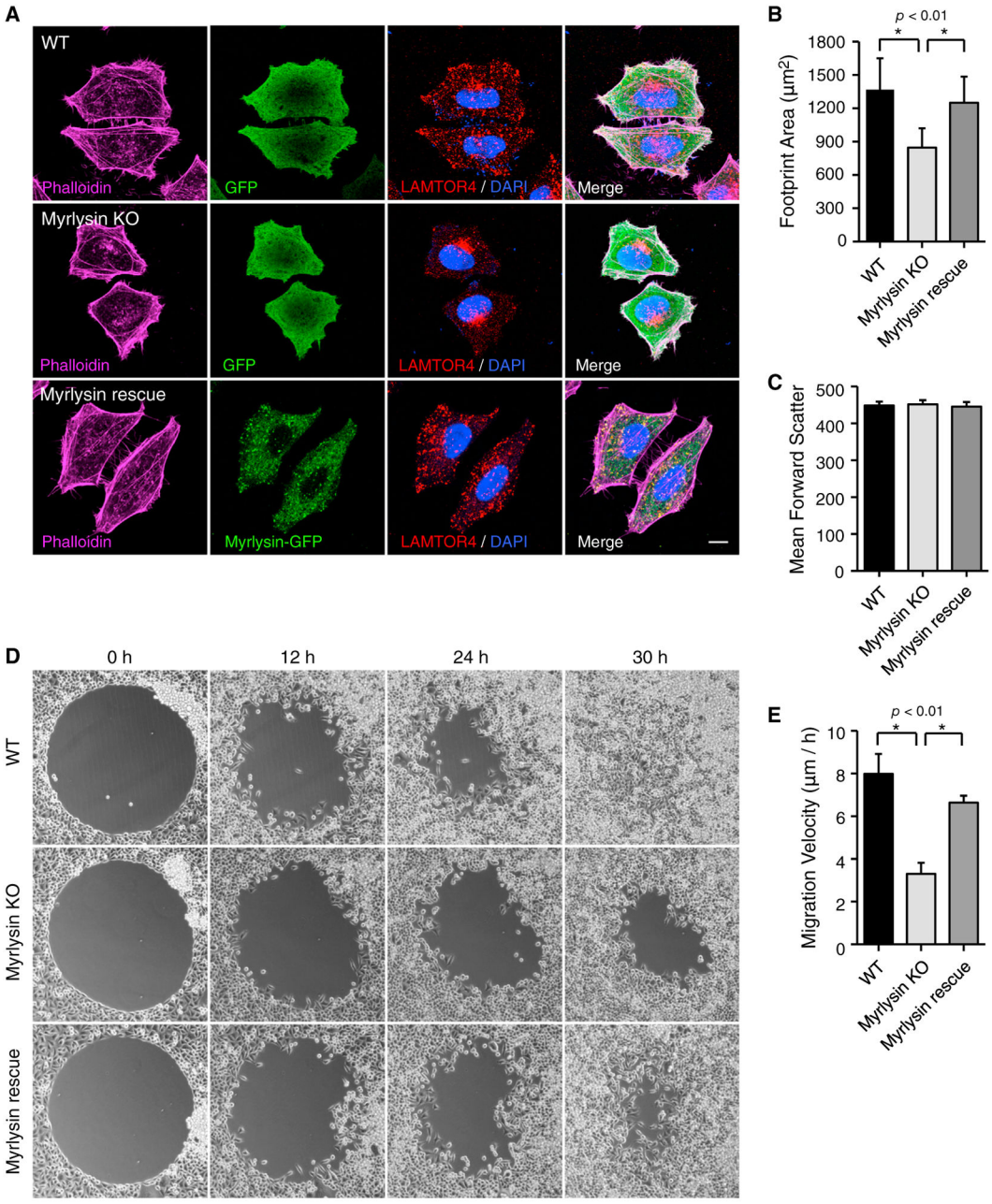

Figure 7. BORC Regulates Cell Spreading and Migration

(A) WT HeLa cells and myrlysin-KO HeLa cells expressing GFP or myrlysin-GFP (rescue) were stained with phalloidin-Alexa 647, antibody to LAMTOR4, and 4′6-diamidino-2-phenylindole, and imaged by confocal microscopy. Scale bar, 10 μm.

(B) The footprint area was calculated using ImageJ from 100 phalloidin-stained cells in each group in (A). Values are mean ± SD. The p values were calculated using Student's t test (right).

(C) WT, myrlysin-KO, and myrlysin-GFP rescue HeLa cells were detached from culture plates using 10 mM EDTA in PBS, and forward-scatter was measured by flow cytometry of 50,000 cells in each group. Error bars indicate the coefficient of variation.

(D) Two-dimensional cell migration was analyzed using a circular gap closure assay. Images were captured at the indicated time points.

(E) The empty area was measured using ImageJ, and cell migration velocity was calculated from the images at 0 and 24 hr in five independent experiments. Values are mean ± SD. The p values were calculated using Student's t test (right). See also Figure S4.